Physics of the Solid State, Vol. 45, No. 2, 2003, pp. 259–265. Translated from Fizika Tverdogo Tela, Vol. 45, No. 2, 2003, pp. 248–253.

DEFECTS, DISLOCATIONS, AND PHYSICS OF STRENGTH

Dislocation-Induced Photoluminescence in Silicon Crystals of Various Impurity Composition

S. A. Shevchenko and A. N. Izotov

Institute of Solid-State Physics, Russian Academy of Sciences, Chernogolovka, Moscow oblast, 142432 Russia

Received May 14, 2002

Abstract—The effect of oxygen on the dislocation-induced photoluminescence (DPL) spectra at 4.2 K is studied in silicon crystals with different impurity compositions subjected to plastic deformation at temperatures above 1000°C. A strong effect of doping impurities on the DPL spectra is observed for concentrations above 10^{16} cm^{-3}. It is shown that the peculiarities of many DPL spectra in silicon can be explained by assuming that the *D*1 and *D*2 lines are associated with edge-type dislocation steps on glide dislocations. © *2003 MAIK "Nauka/Interperiodica".*

1. INTRODUCTION

Dislocation-induced photoluminescence (DPL) in silicon at 4.2 K is characterized by the lines *D*1 (0.807 eV), *D*2 (0.870 eV), *D*3 (0.935 eV), and *D*4 (1.00 eV) [1]. The *D*4 line and *D*3 line (TO phonon replica of the *D*4 line) are attributed to the emission of regular segments of split 60° dislocations [2–4]. The interest in the origin of the *D*1 and *D*2 lines, which has not been clarified completely, is due to the possible application of this radiation in optoelectronics, which was demonstrated in [4].

It is well known that *D*1 and *D*2 lines are observed in silicon crystals subjected to plastic deformation at temperatures $T < 900$°C and then annealed in the temperature range 400–1200°C. The analysis of the conditions for the emergence and disappearance of these lines carried out in [2, 5–10] indicates their possible relation to translational-symmetry violation at dislocations, i.e., to specific step-type defects and dislocation nodes.

On the other hand, *D*1 and *D*2 lines of appreciable intensity have been detected in initial Czochralski-grown silicon (Cz-Si) crystals after annealings facilitating the nucleation and growth of oxygen precipitates [11–13]. Oxygen precipitation is accompanied by the generation of interstitial Si_i atoms and the formation of interstitial dislocation loops, whose plane is perpendicular to the Burgers vector **b**: partial Frank dislocation loops ($\mathbf{b} = (a/3)\langle 111\rangle$, with a being the lattice constant) and perfect prismatic dislocation loops [$\mathbf{b} = (a/2)\langle 110\rangle$]. As a result of absorption of excess Si_i atoms, these dislocations climb through the formation and displacement of edge steps in the plane of the loop [14]. The *D*1 and *D*2 lines detected in the recrystallized (100) Si layers after annealing at 1100°C in a chlorine-containing atmosphere are attributed to a three-dimensional network of pure edge dislocations [15]. The occurrence of a change in the defect structure of these layers upon annealing is due to the expansion of perfect prismatic loops as a result of climbing and to the elastic interaction between large loops that approach one another.

Transmission electron-microscopic studies revealed that these dislocation loops in silicon are effective getters of transition metals [16–18]. In silicon crystals grown through crucibleless floating-zone melting (FZ-Si) intentionally contaminated with copper, colonies of copper precipitates were observed in the area swept by helicoidal dislocations [16, 17] formed from gliding screw dislocations with edge steps as a result of climbing of these steps [14]. This fact, as well as a discrete arrangement of copper precipitates on partial Frank dislocations [17], allows us to consider edge steps as defects that facilitate the nucleation of copper precipitates. According to [18–20], oxygen precipitates in the form of SiO_x polyhedrons ($1 < x < 2$) are formed at temperatures above 900°C in some regions on dislocations and at the nodes of a dislocation network.

The above arguments suggest that the *D*1 and *D*2 lines in plastically deformed crystals are associated with edge-type steps on gliding dislocations, as well as with dislocation nodes, i.e., with defects near which precipitates of various impurities nucleate. The maximum decrease in the concentration of interstitial oxygen atoms as a result of precipitation occurs at 1050°C [21]; therefore, the effect of oxygen on the DPL spectrum may be pronounced most strongly in this temperature region. In order to verify this hypothesis, we studied DPL spectra in silicon crystals with different concentrations of oxygen and doping impurities deformed at $T > 1000$°C.

1063-7834/03/4502-0259$24.00 © 2003 MAIK "Nauka/Interperiodica"

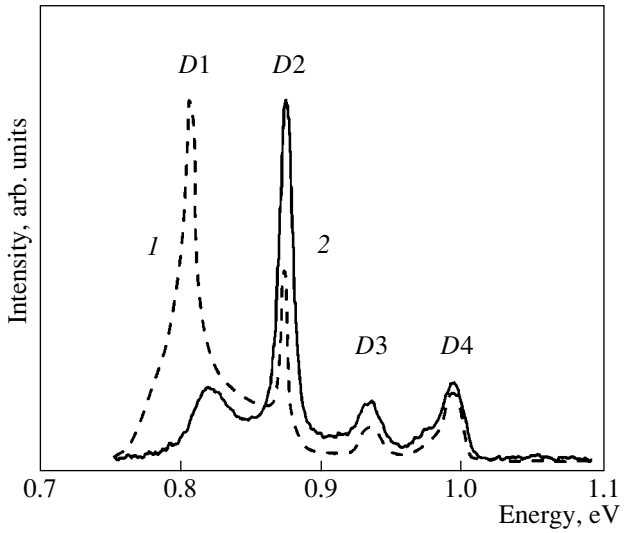

Fig. 1. DPL spectra recorded at 4.2 K in (*1*) *n*-type FZ-Si ($N_P = 6 \times 10^{13}$ cm^{-3}) and (*2*) *n*-type Cz-Si crystals ($N_P = 2 \times 10^{14}$ cm^{-3}. The dislocation density N_D is equal to (*1*) 4×10^6 and (*2*) 6×10^6 cm^{-2}; $T_d = 1050$°C.

2. EXPERIMENTAL TECHNIQUE

Experiments were carried out on silicon single crystals doped with boron (*p* type) or phosphorus (*n* type) with different oxygen contents and with a growth-dislocation density below 100 cm^{-2}. The boron concentration N_B and the phosphorus concentration N_P were varied in the intervals $10^{12} < N_B < 1.6 \times 10^{16}$ cm^{-3} and $6 \times 10^{13} < N_P < 8 \times 10^{16}$ cm^{-3}. In FZ- and Cz-Si crystals, the oxygen concentration was $\sim 1 \times 10^{17}$ and $\sim 1 \times 10^{18}$ cm^{-3}, respectively. In crystals with N_B, $N_P > 10^{16}$ cm^{-3}, the carbon concentration amounted to 10^{17} cm^{-3}. These data were obtained from the infrared absorption spectra. Chemically polished parallelepipeds with dimensions of $3.2 \times 3.4 \times 11$ mm were deformed in a vacuum of ~7 Pa through compression along the longest edge ($\langle 123 \rangle$ direction) at various temperatures from the interval $1050 \le T_d \le 1200$°C up to strains $0.5\% < \delta < 30\%$ [6]. After deformation, the crystals were unloaded and cooled slowly (at a rate of less than 10 deg/min) to room temperature, which facilitated the formation of an equilibrium dislocation structure in the samples. The dislocation density was determined from etching pits on the {111} face.

The dislocation structure produced by high-temperature deformation was studied earlier in [6]. This structure is formed not only through the motion of dislocations in the slip plane but also through their leaving this plane due to cross glide of screw segments and climb of edge segments. In the crystals with the above-mentioned orientation, for moderate deforming stresses τ, only one glide system operates and part of the isolated dislocations takes the form of rectilinear (regular) segments of screw- or 60° dislocations separated by kinks and jogs. Activation of other glide systems at higher values of τ and the interaction of dislocations facilitate the formation of a cellular structure and the emergence of dislocation nodes. For $\delta > 20\%$, regular segments of screw- and 60° dislocations form a network whose connectivity increases with δ.

The PL spectra were measured at 4.2 K in the energy range 0.8–1.2 eV using a technique employed earlier in [5–7, 10]. The power density of excitation of nonequilibrium electrons and holes by Ar laser radiation at a wavelength of 488.8 nm was 2 mW/cm^2.

3. RESULTS

According to [7], the shapes of the DPL spectra in FZ- and Cz-Si crystals of type *p* with $N_B = 4 \times 10^{13}$ cm^{-3} deformed at 1050°C differ significantly for relatively small densities of introduced dislocations ($N_D < 2 \times 10^7$ cm^{-2}). The DPL spectra of FZ- and Cz-Si crystals (with different types and concentrations of doping impurities) deformed at $T \ge 1050$°C are presented below. It was found that an analogous difference is also observed in the DPL spectra of FZ- and Cz-Si crystals of type *n* with $N_P \le 2 \times 10^{14}$ cm^{-3}. An *n*-type FZ-Si sample (curve *1* in Fig. 1, $N_P = 6 \times 10^{13}$ cm^{-3}) is characterized by a typical DPL spectrum containing *D*1–*D*4 lines attributed to dislocations. In the spectrum of an *n*-type Cz -Si sample (curve *2*, $N_P = 2 \times 10^{14}$ cm^{-3}), instead of the *D*1 line, a broadened line with maximum energy $E_m = 0.82$ eV appears, which is displaced to $E_m = 0.83$ eV for $N_D \sim 1.5 \times 10^7$ cm^{-2}. A specific DPL spectrum is observed for Cz-Si samples of the *n* and *p* types, deformed in the temperature range $1050 \le T_d \le 1200$°C, with a donor concentration $N_P \le 2 \times 10^{15}$ and acceptor concentration $N_B \le 1.6 \times 10^{16}$ cm^{-3}, respectively.

The effect of dislocation density on the PL spectra is investigated in the *p*-type Cz-Si crystals with $N_B = 1.6 \times 10^{16}$ cm^{-3} ($T_d = 1170$°C; Fig. 2). As in [7], an increase in the dislocation density for $N_D < 2 \times 10^7$ cm^{-2} intensifies the PL in the vicinity of the *D*1 and *D*2 lines. However, for $N_D > 2 \times 10^7$ cm^{-2}, radiation appears with energy $E_m = 0.807$ eV, corresponding to the *D*1 line; the intensity of this radiation increases with N_D at a much higher rate than the intensity of the *D*2 line. Consequently, the broad *D*1 line (curve 3, $N_D \sim 10^9$ cm^{-2}) dominates in the PL spectra for $N_D \sim 10^8$–10^9 cm^{-2}. Samples *1–3* display an increase in the radiation intensity at energies 0.95–0.97 eV (inset to Fig. 2), which is often observed in the form of a small step on the long-wavelength wing of the *D*4 line (see, e.g., Fig. 1).

Figure 3 shows the DPL spectra in *n*-type Cz-Si crystals doped with phosphorus ($N_P = 2.6 \times 10^{16}$cm^{-3}, $T_d = 1170$°C). For samples with $N_D \sim 10^7$ cm^{-2}, quite

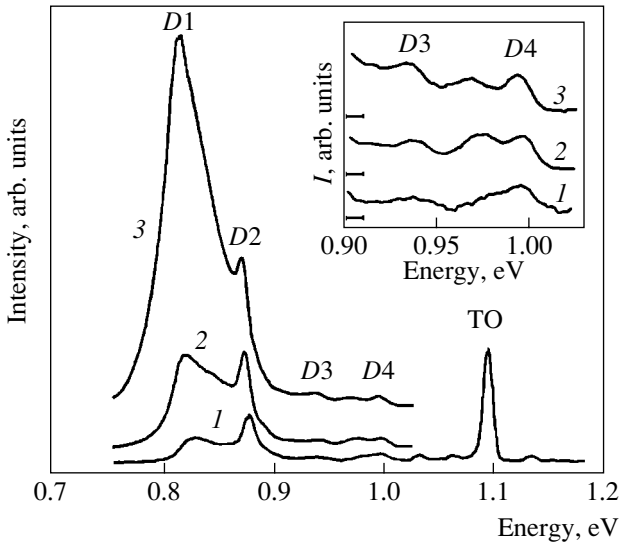

Fig. 2. DPL spectra recorded at 4.2 K in *p*-type Cz-Si crystals ($N_B = 1.6 \times 10^{16}$ cm^{-3}) for different dislocation densities N_D: (*1*) 8×10^6, (*2*) higher than 2×10^7, and (*3*) ~10^9 cm^{-2}. T_d = 1170°C.

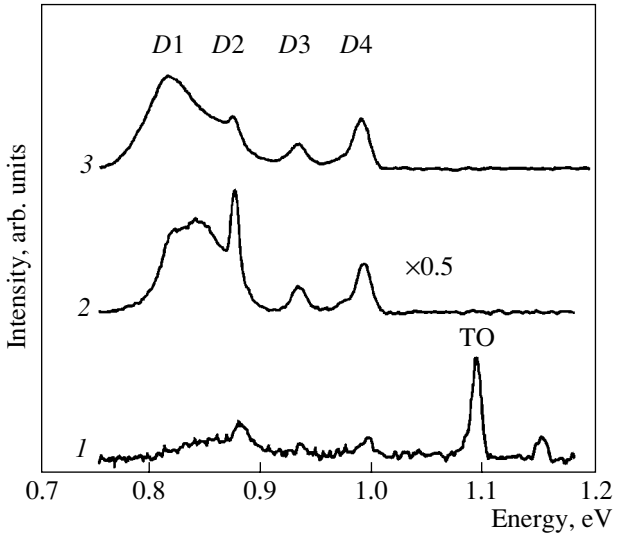

Fig. 3. DPL spectra recorded at 4.2 K in *n*-type Cz-Si crystals ($N_P = 2.6 \times 10^{16}$ cm^{-3}) for different dislocation densities N_D: (*1*) 1.2×10^7, (*2*) ~10^8, and (*3*) ~10^9 cm^{-2}. T_d = 1170°C.

small peaks are detected in place of the *D*2, *D*3, and *D*4 lines (curve *1*). A further increase in N_D facilitates a rise in the intensity of the *D*1–*D*4 lines. A wide emission band on the left of the *D*2 line (curve *2* in Fig. 3) indicates that samples with $N_D \sim 10^8$ cm^{-2} display emissions with E_m = 0.807 and 0.830 eV, which are of approximately equal intensities. In the sample with δ = 25% (curve *3* in Fig. 3), emission in the vicinity of the *D*1 line becomes dominant; its integrated intensity (I_{D1}), reduced to the same measurement conditions, turned out to be an order of magnitude lower than that in sample *3* (Fig. 2).

Since the concentrations of oxygen and carbon are virtually identical in the initial Cz-Si crystals of the *n* and *p* types with N_B, $N_P > 2 \times 10^{16}$ cm^{-3}, the considerable decrease in radiation intensity in the vicinity of the *D*1 and *D*2 lines observed in *n*-type Cz-Si samples could be due to the type of the doping impurity involved. For this reason, DPL spectra were also studied in *n*-type FZ-Si crystals with $N_P = 8 \times 10^{16}$ cm^{-3}. In the sample with $N_D = 3 \times 10^6$ cm^{-2}, the dislocation-induced PL is not detected. A very weak *D*2 line and quite intense *D*3 and *D*4 lines are observed for $N_D = 1.5 \times 10^7$ cm^{-2} (curve *1* in Fig. 4). A 30-min annealing of the sample at T_0 = 700–800°C does not affect the spectrum. At higher values of N_D, emission in the vicinity of the *D*1 and *D*2 lines is detected (curve *2*), but the values of I_{D1} are also an order of magnitude smaller than those for sample *3* (Fig. 2).

It should be noted that in samples with different oxygen contents (Figs. 2–4), an increase in N_D from 10^7 to 10^9 cm^{-2} does not lead to a large difference in the values of I_{D4} (these quantities differ by only a factor of several units). Consequently, the comparable values of I_{D1} and I_{D4} in samples with $\delta > 20\%$ (Figs. 3, 4) reflect a decrease in the effectiveness of emission in the vicinity of the *D*1 line.

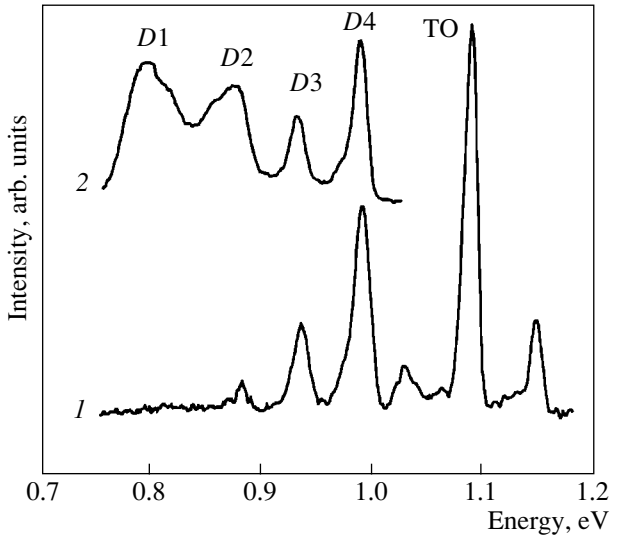

Fig. 4. DPL spectra recorded at 4.2 K in *n*-type FZ-Si crystals ($N_P = 8 \times 10^{16}$ cm^{-3}) for different dislocation densities N_D: (*1*) 1.5×10^7 and (*2*) ~10^9 cm^{-2}. T_d = 1050°C.

For FZ- and Cz-Si samples with N_B, $N_P > 10^{16}$ cm^{-3} and $N_D \le 1.5 \times 10^7$ cm^{-2} (Figs. 2–4), the emission of a TO exciton, its phonon replica, and the emission of a TA exciton were detected in [10] for $E > 1$ eV.

Thus, the above results indicate specific changes in the DPL spectra upon an increase in the oxygen, boron, and phosphorus concentrations.

4. DISCUSSION

4.1. DPL Spectra for Energies E < 0.9 eV

A comparative analysis of the DPL spectra in FZ- and Cz-Si crystals carried out by us earlier [7] and in this work made it apparent that the broadened line with E_m = 0.82–0.83 eV is a characteristic feature of deformed Cz-Si crystals with $N_D < 2 \times 10^7$ cm^{-2}. The $D1$ line appears in the DPL spectrum after annealing of these crystals at 1070°C for t_0 = 30 min, followed by slow cooling to room temperature [7], or after the introduction of a large number of dislocations ($N_D = 2 \times 10^7$ cm^{-2}, Fig. 2). These facts correlate with results obtained by other authors. The $D1$ line is shifted towards higher energies under uniaxial elastic deformation of samples with introduced dislocations [22] or after their annealing in oxygen at 750°C [23]. In *n*-type Cz-Si samples deformed at 900°C ($N_d = 2 \times 10^{14}$ cm^{-3}, $N_D \sim 10^9$ cm^{-2}), the emission in the vicinity of the $D1$ line depends on the cooling rate of the samples after annealing at 1200°C [24]. In the case of slow cooling, the $D1$ line is replaced by a broad step adjoining the long-wavelength wing of the $D2$ line and falling off steeply for $E < 0.82$ eV; after annealing, $D1$ and $D2$ lines of approximately equal intensities are detected. The broad band with a peak at $E \approx 0.82$ eV and the $D2$–$D4$ lines are observed after rapid (t_d = 15 min, $N_D = 5 \times 10^5$ cm^{-2}) deformation of Cz-Si samples at 700°C [9], while for t_d = 14 h, DPL disappears completely.

The sum of these factors indicates that oxygen precipitation in Cz-Si crystals is a possible reason for the strong effect of the conditions of sample preparation on radiation in the vicinity of the $D1$ line.

We assume that, in the case of slow cooling of *n*- and *p*-type Cz-Si samples (Figs. 1, 2) followed by deformation, interstitial oxygen atoms precipitate on the available growth precipitates and in the vicinity of dislocation steps. The mismatching of the molar volumes of the matrix and the precipitates gives rise to elastic stresses whose magnitude are maximal for the plane precipitate and decreases by an order of magnitude at a distance ~10^{-5} cm [11]. The effect of elastic stresses on the position of the $D1$ line [22, 23] allows us to attribute the emergence of radiation with E_m = 0.82–0.83 eV (Figs. 1, 2; see also [9, 24]) to the presence of the steps responsible for the $D1$ line in the vicinity of precipitates.

The emergence of the $D1$ line in the spectra of deformed Cz-Si samples after annealing at 1070°C [7] is probably due to the removal of steps from precipitates as a result of dislocation climbing upon absorption of interstitial silicon atoms generated during precipitate growth. The detachment of 60° dislocations from oxygen precipitates through climbing was observed in Cz-Si crystals at 900°C [20]. The transformation of a line with E_m = 0.818 eV into a $D1$ line (E_m = 0.807 eV) after long-term annealing of Cz-Si crystals correlates with the removal of dislocation loops from precipitates [13], while the excitation of the $D1$ line (reported in [24]) after annealing at 1200°C followed by quenching correlates with precipitate dissolution [21].

The number of steps increases with N_D as a result of moving-dislocations overcoming obstacles in the form of impurity atoms, precipitates, and forest dislocations, as well as due to the generation of steps during the formation of dislocation nodes [14]. According to [6], the separation between the nodes in dislocation networks in samples subjected to strong plastic deformations ($\delta \sim$ 20–30%) amounts to 50–500 nm. Assuming that the number of steps exceeds the number of nodes, we take a value of 50 nm for the mean distance between the steps. In this case, for the dislocation density $N_D \sim 10^9$ cm^{-2}, we obtain the step concentration ~10^{14} cm^{-3}, which is an order of magnitude higher than the maximum possible concentration of precipitate nuclei in Cz-Si crystals with $N_O \sim 10^{18}$ cm^{-3} [25]. At a given temperature T_0, this concentration is determined by the annealing time for which the oxygen diffusion length becomes comparable with the mean distance between precipitates. In this case, the growth of existing precipitates is more probable than the nucleation of new precipitates; i.e., the number of steps near which no precipitates are formed increases with N_D. For this reason, the $D1$ line emerges in the DPL spectrum for $N_D > 10^7$ cm^{-2}, with its intensity increasing with δ (Fig. 2).

The sensitivity of the $D1$ line to oxygen, the minimal energy barrier for the formation of copper precipitates at perfect prismatic dislocations [17], and the formation of helicoidal dislocations during oxygen precipitation in silicon [20] indicate that the edge steps associated with the $D1$ line could be localized at screw dislocations. The $D2$ line can be attributed to edge-type steps at 60° dislocations. Regular segments of a screw dislocation are split into two 30° partial dislocations, while 60° dislocations are split into 30° and 90° partial dislocations. Ruptured bonds of both partial dislocations are reconstructed (pairwise closed) and do not create any deep states in the band gap of silicon. Two quasi-one-dimensional bands that are split off from the conduction band (empty E_{Dc} band) and from the valence band (filled E_{Dv} band) and that are located at a distance of ~0.07 eV from the edges of their parent bands are associated with the deformation potential of 90° partial dislocations. Consequently, deep states

associated with edge steps or dislocation nodes and manifested in PL may be due to the presence of silicon atoms with unsaturated bonds.

A considerable decrease in the PL intensity in the vicinity of the *D*1 and *D*2 lines in deformed *n*-type Cz- and FZ-Si samples with $N_P > 10^{16}$ cm^{-3} (Figs. 3, 4) relative to *p*-type Cz-Si samples (Fig. 2) correlates with the suppression of oxygen precipitation in *n*-type Cz-Si samples as a result of strong doping by Group V impurities (in contrast to doping with boron) [26], as well as with the difference between the effects produced by boron and phosphorus on the mobility of dislocations in Si [27]. The problem of interaction of technological impurities (nitrogen, oxygen, carbon) and some other doping impurities from Groups III and V with cores of 90° partial dislocations in silicon was investigated theoretically in [28]. The decelerating effect of oxygen on the motion of dislocations was attributed to accelerated diffusion of interstitial oxygen atoms O_i along the cores of these dislocations and to the formation of a stable complex of two O_i atoms in the region of extension. The As, B, N, and P impurities, in contrast to oxygen, interact chemically with the core of a 90° partial dislocation, thus rupturing the reconstructed bonds, and with a reconstruction defect in this core (soliton). A soliton is a solitary Si atom with three saturated bonds and one unsaturated bond situated at the boundary between reconstructed regular segments of partial dislocations with different phases. Consequently, a phosphorus atom in the core of a partial dislocation can replace, for example, a Si atom with (a) four or (b) three saturated bonds (during its interaction with a soliton). In case (a), there is a shallow donor level of phosphorus and a deep level of the soliton in the band gap, while in case (b), we are left only with a shallow level (associated with a pair of valence electrons in phosphorus) near the top of the valence band or in the valence band; i.e., passivation of unsaturated bonds of the soliton takes place. According to [28], the soliton being pinned at these impurities (case b) is more advantageous from the energy point of view. As a result, dislocation-pinning centers with high binding energies are formed ($E^* = 2.3$–2.5 eV for As, B, and P and 3.4 eV for N). Such values of E^* are due to a change in the structure of chemical bonds in the core and to the necessity of their switching during the motion of dislocations (otherwise, an impurity atom would follow the dislocation).

The chemical interaction of phosphorus with edge steps may also lead to passivation of their electric activity, which explains the considerable decrease in the intensity of the *D*1 and *D*2 lines in *n*-Si with $N_P > 10^{16}$ cm^{-3} (Figs. 3, 4). The high intensity of the *D*1 line in *p*-type Cz-Si (Fig. 2) and the above-mentioned results [26, 27] indicate that the behavior of boron does not match the predictions made in [28]. In real crystals, the formation of impurity complexes depends, in particular, on the charge state of doping impurities and intrinsic point defects, the concentration of technological impurities, and the probability of formation and the thermal stability of clusters SiO_x, B_2O_3, P_2O_5, etc. [26]. Boron and phosphorus atoms differ in the value of the covalent radius (0.86, 1.10, and 1.18 Å for B, P, and Si, respectively) and in the sign of the ions at $T \sim 1000$°C in the samples under investigation (positive for P and negative for B). In the case of doping with boron, the nucleation of oxygen precipitates near edge steps is apparently more advantageous from the energy viewpoint, while in the case of doping with phosphorus, the chemical interaction of phosphorus with the steps dominates.

In the framework of this hypothesis, the reason for the emergence of the *D*1 and *D*2 lines in the presence of transition metals is associated in [29] with the formation of edge steps due to dislocation climb during diffusion or precipitation of these impurities.

4.2. DPL Spectra for Energies E > 0.9 eV

In deformed *p*-type Cz-Si samples (Fig. 2), the *D*4 line ($E_m = 0.998 \pm 0.001$ eV) is attributed to the emission of regular segments of 60° dislocations with an equilibrium value of the stacking fault width Δ_0. This radiation is the result of recombination of nonequilibrium electrons and holes trapped in quasi-one-dimensional bands E_{Dc} and E_{Dv}, respectively. The deformation potential of a 30° partial dislocation plays the role of a weak perturbation whose magnitude depends on the distance between partial dislocations, i.e., on the value of Δ. This parameter affects the depths of the bands E_{Dc} and E_{Dv} and, accordingly, the energy of radiation. The value of Δ can be changed, for example, by cooling a deformed sample to room temperature under a large load [2, 3]. Such a sample acquires regular segments of 60° dislocations with nonequilibrium values of Δ, while the DPL spectra of Si acquire a series of narrow lines (instead of the *D*4 line). For $\Delta > \Delta_0$, each value of Δ corresponds to a narrow line with a value of $E_m > 1.00$ eV, which increases discretely with Δ, while for $\Delta < \Delta_0$, the values of E_m decrease discretely in the interval 1.00–0.93 eV. Thus, radiation with $E_m = 0.95$–0.97 eV in *p*-type Cz-Si samples with an equilibrium dislocation structure (see the inset to Fig. 2) falls in the energy range corresponding to segments of 60° dislocations with nonequilibrium values of $\Delta < \Delta_0$. This could mean that, in addition to regular segments of 60° dislocations with equilibrium values of Δ_0, such samples also contain regular segments with $\Delta_{0e} < \Delta_0$.

An analysis of the DPL spectra of plastically deformed Ge crystals with an equilibrium dislocation structure [30] reveals that the value of $E_m = 0.513$ eV for band 1, associated with 60° dislocations, corresponds to regular segments of 60° dislocations with an

equilibrium splitting Δ_0 in only one sample. For the remaining samples, lower values of E_m = 0.497–0.508 eV are observed.

The electron-microscopic images presented in [31] show that regular segments of glide dislocations in Ge samples with an equilibrium dislocation structure are characterized by different lengths and values of Δ. Regular segments with $L > L_c$ correspond to the value Δ_0, while those with $L < L_c$ correspond to the value $\Delta_{0e} < \Delta_0$. The critical length L_c amounts to ~100 nm; i.e., the relation $L > (20–30)\Delta_0$ holds for long segments ($L > L_c$), while the minimal values Δ_{0e} correspond to segments with $L \sim 30$ nm.

The above results lead to the conclusion that the spectral composition of PL in Si and Ge associated with an equilibrium ensemble of regular segments of 60° dislocations is determined by the distribution of these segments over the lengths and the values of Δ. A higher intensity of radiation with E_m = 0.95–0.97 eV (due to an increase in the number of 60° dislocations with lengths $L < L_c$) in *p*-type Cz-Si samples with $N_D > 10^7$ cm^{-2} correlates with the presence of oxygen precipitates.

In the spectra of deformed FZ- and Cz-Si samples doped with phosphorus with $N_P > 10^{16}$ cm^{-3}, the *D*4 line is characterized by the value $E_m = 0.988 \pm 0.001$ eV (Figs. 3, 4), which is 10 eV lower than the values of E_m for crystals with a different level of doping (Figs. 1, 2). In analogy with the above arguments, we assume that these values of E_m are due to a decrease in the lengths of the majority of regular segments of 60° dislocations to values $L < L_c$. This range of L values is apparently determined by the number of steps whose electrical activity is passivated by phosphorus.

5. CONCLUSIONS

Thus, the hypothesis on the relation between the *D*1 and *D*2 lines and the edge-type steps makes it possible to explain specific features of the DPL spectra in Si crystals with a large oxygen content. Oxygen precipitates formed in deformed *p*-type Cz-Si crystals with dislocations affect the number and the radiation energy of the steps separating regular segments, as well as the length of these segments. The quenching of the *D*1 and *D*2 lines in the case of an elevated phosphorus concentration is, in all probability, a manifestation of the chemical interaction of phosphorus with the steps. Low solubility of oxygen and transition metals at room temperature and their effective interaction with the steps facilitate concentration of these impurities in individual regions on dislocations, which causes carrier recombination to occur at quasi-one-dimensional dislocation segments and defects separating them.

ACKNOWLEDGMENTS

The authors are grateful to V.V. Kveder, V.P. Kisel', and A.I. Kolyubakin for useful discussions; E.A. Steinman for his interest in this work and for discussions of the results; and to A.V. Bazhenov for determining the oxygen and carbon concentration in the initial crystals.

This study was supported by the Russian Foundation for Basic Research, project nos. 00-15-96703 and 02-02-17024.

REFERENCES

1. N. A. Drozdov, A. A. Patrin, and V. D. Tkachev, Pis'ma Zh. Éksp. Teor. Fiz. **23**, 651 (1976) [JETP Lett. **23**, 597 (1976)].
2. R. Sauer, C. Kisielowski-Kemmerich, and H. Alexander, Appl. Phys. A **36**, 1 (1985).
3. A. N. Izotov, A. I. Kolyubakin, S. A. Shevchenko, and E. A. Steinman, Phys. Status Solidi A **130**, 193 (1992).
4. V. V. Kveder, E. A. Steinman, S. A. Shevchenko, and H. G. Grimmeiss, Phys. Rev. B **51**, 10520 (1995).
5. A. N. Izotov and E. A. Stienman, Phys. Status Solidi A **104**, 777 (1987).
6. S. A. Shevchenko, Yu. A. Ossipyan, T. R. Mchedlidze, *et al.*, Phys. Status Solidi A **146**, 745 (1994).
7. S. A. Shevchenko and A. N. Izotov, Phys. Status Solidi A **138**, 665 (1993).
8. T. Sekiguchi and K. Sumino, J. Appl. Phys. **79**, 3253 (1996).
9. O. V. Feklisova, G. Mariani-Reguta, B. Pichaud, and E. B. Yakimov, Phys. Status Solidi A **171**, 341 (1998).
10. E. A. Steinman, V. I. Vdovin, T. G. Yugova, *et al.*, Semicond. Sci. Technol. **14**, 582 (1999).
11. W. Wijaranakula, J. Appl. Phys. **72**, 4026 (1992).
12. C. Clayes, E. Simoen, and J. Vanhellemont, J. Phys. III **7**, 1469 (1997).
13. S. Pizzini, M. Guzzi, E. Grilli, and G. Borionetti, J. Phys.: Condens. Matter **12**, 10131 (2000).
14. J. Friedel, *Dislocations* (Pergamon, Oxford, 1964; Mir, Moscow, 1967).
15. V. I. Vdovin, N. A. Sobolev, A. M. Emel'yanov, *et al.*, Izv. Ross. Akad. Nauk, Ser. Fiz. **66**, 279 (2002).
16. H. Gotschalk, Phys. Status Solidi A **137**, 447 (1993).
17. B. Shen, T. Sekiguchi, J. Jablonski, and K. Sumino, J. Appl. Phys. **76**, 4540 (1994).
18. K. Sumino, Phys. Status Solidi A **171**, 111 (1999).
19. A. Cavallini, M. Vandini, F. Cirticelli, and A. Armigliato, Inst. Phys. Conf. Ser. **134**, 115 (1993).
20. K. Minova, I. Yonenaga, and K. Sumino, Mater. Lett. **11**, 164 (1991).
21. H. Möller, L. Long, M. Werner, and D. Yang, Phys. Status Solidi A **171**, 175 (1999).

22. A. N. Drozdov, A. A. Patrin, and V. D. Tkachev, Phys. Status Solidi B **83**, K137 (1977).
23. A. N. Drozdov, A. A. Patrin, and V. D. Tkachev, Phys. Status Solidi A **64**, K63 (1981).
24. A. N. Izotov and E. A. Steinman, Fiz. Tverd. Tela (Leningrad) **28**, 1172 (1986) [Sov. Phys. Solid State **28**, 655 (1986)].
25. A. Borghesi, B. Pivac, A. Sassela, and A. Stella, J. Appl. Phys. **77**, 4169 (1995).
26. S. Hahn, F. A. Ponce, W. A. Tiler, *et al.*, J. Appl. Phys. **64**, 4454 (1988).
27. M. Imai and K. Sumino, Philos. Mag. A **47**, 599 (1983).
28. R. Jones, A. Umerski, P. Sitch, *et al.*, Phys. Status Solidi A **138**, 369 (1993).
29. E. C. Lightowlers and V. Higgs, Phys. Status Solidi A **138**, 665 (1993).
30. A. I. Kolyubakin, Yu. A. Osip'yan, S. A. Shevchenko, and E. A. Steinman, Fiz. Tverd. Tela (Leningrad) **26**, 677 (1984) [Sov. Phys. Solid State **26**, 407 (1984)].
31. G. Packeiser and P. Haasen, Philos. Mag. **35**, 821 (1977).

Translated by N. Wadhwa